Available online at www.sciencedirect.com

ScienceDirect

Procedia Structural Integrity 12 (2018) 457–470

Structural Integrity Procedia

www.elsevier.com/locate/procedia

AIAS 2018 International Conference on Stress Analysis

Dies for pressing metal powders to form helical gears

Enrico Armentani[a,*], Angelo Mattera[b], Raffaele Sepe[a], Luca Esposito[a], Francesco Naclerio[b], Gian Filippo Bocchini[c]

[a]*University of Naples Federico II, P.le V. Tecchio 80, 80125 Naples, Italy*
[b]*Officine Meccaniche Pontillo S.r.l., Via Aquino, 84018 Scafati (SA) Italy*
[c]*Powder metallurgy consultant, Rapallo, GE, Italy*

Abstract

This work concerns the realization of dies to produce helical gears by metal powder compaction. Due to the helicoidal geometry of the cylindrical gears, the punch, in addition to the axial motion, must necessarily rotate to "cross" the die. The innovative idea is to design a perfectly functioning system that can generate any helix angle (β) in the range of interest 0°-30°, using the simple contact between punch and die cavity during the rotation. First of all, the punch-die system was treated as a self-locking screw to determine the maximum ß-value at which punch could be clamped inside the die during pressing. The analysis encouraged the execution of experimental tests related to a die with β = 5°, obtaining excellent results. Subsequently, FEM (Finite Element Method) analyses were performed on the static behavior of the die, subjected to the pressures exerted by powder and shrink-fitting ring, for three different β-values: 5°, 18° and 30°. The results obtained for the latter two angles were compared with those related to the die with β equal to 5°, considered valid thanks to experimentation, in order to theoretically verify the correct functioning even of dies with larger angles.

Peer-review under responsibility of the Scientific Committee of AIAS 2018 International Conference on Stress Analysis.

Keywords: Powder Metallurgy, Compaction, Die, FEM analysis, Interference, Shrink fitting, Sintered helical gears

* Corresponding author. Tel.: +39-081-768-2450; fax: +39-081-768-2172.
E-mail address: enrico.armentani@unina.it

10.1016/j.prostr.2018.11.072

1. Introduction

System geometry, interference fit, material selection and stress levels are the main parameters to be properly analysed when designing shrink-fitted dies to be used for metal powder compaction. Various comparisons between analytical and numerical calculations, Armentani et al. (2002), Armentani et al. (2003), showed that the FEM (Finite Element Method) approach is the most suitable to establish the correct interferences and to evaluate the stress levels, at rest and at work. For instance, in the case of warm compaction dies with hard metal inserts, the highest stresses on both items, liner and shrink-fitting ring, are present at room temperature, i.e. when the die is not subjected to internal pressure at about 130 ÷ 150 °C, Armentani et al. (2007). Knowledge of the acting stresses in any condition is a guarantee against operating failures, Cricrì and Perrella (2016), but it is not sufficient to assure the maximum useful life, and the minimum unit cost per part as well. These factors depend on die structure, die dimensioning, compaction pressure, powder type, part tolerance and wear rate. A "precision" die dimensioning may be the key factor when different PM (Powders Metallurgy) manufacturers are competing each other. Such a precise dimensioning must include, at least, the increase of inner die dimensions under the radial compaction pressure, the compact spring-back on ejection, the allowance for dimensional changes on sintering. Since many part producers are trying to use powder mixes with null dimensional changes, the correct prediction of die size expansion under pressure becomes a basic parameter. In addition, it cannot be excluded that this expansion, which is varying along the die height, may affect ejection pressure and compact spring-back. The favor encountered by sinter hardening materials is another reason for improving the precision of die dimensioning. Last but not least, some powder producers are striving to reduce the scattering of dimensional changes on sintering of their products. For all the listed grounds, a specific study on the relationship between die structure and elastic behavior under compaction stresses seems to be useful to PM part manufacturers. The elastic increase of the inner dimensions of a shrink-fitted die depends on the radial pressure acting at compaction end, inner and outer dimensions, thickness of each item – if they are made of different materials – and working temperature, which modifies the elastic parameters of constituting materials. Since the inner die profile and dimensions are attained after shrink fitting, by grinding or by EDM (Electrical Discharge Machining), the effect of interference should be excluded.

Armentani et al. (2008) carried out FEM analyses of different shelf dies, to find stress distribution and deformation pattern, taking into account different die geometries, relative interferences and three different nucleus materials. The stress levels due to compaction of flanged parts inside shelf dies can be too high to be compensated by pre-stressing through shrink fitting, within the investigate range of compact shapes. The increasing of radiuses consent to reduce the stress levels.

Armentani et al. (2012) investigated, by analytical and FEM calculations, the behavior of twice shrink fitted dies, with circular profiles, which are relatively expensive and complex to build, in order to optimize dimensions and stresses, especially in case of die size limitations in the tool holder of the press.

Armentani et al. (2013) also investigated the stress-strain states in straight toothed wheels. A systematic study on the possible effects of some design parameters (modulus, teeth number, top fillet radius of the gear, relative interference) was carried out by FEM.

In this study, by applying results obtained in the previous ones, dies for metal powder compaction, suitable to form sintered helical gears, have been characterized by FEM analyses. Stress levels should be lower than yielding ones, and also displacements should be small to avoid problems in the compact ejection. Finally, experimental tests confirm the correct functioning, without problems related to the die slip-off during the compact extraction.

2. Device description

Today, in the industrial practice, there are different devices to form helical gears by metal powder compaction. These devices are used to form green parts, to be consolidated by sintering, if required with adjacent hub portions. The hub portions may, also, carry gear teeth, or be smooth at the outer profile, or have positive engagement elements such as grooves, wedge-like projections, splines and the like.

Officine Meccaniche Pontillo has developed, in collaboration with Sacmi Imola S. C., a new device that is able to form helical gears, with helix angle in the range 0° - 30° through pressing of powdered metal, removing all the reset

operations needed to get new wheels with a different pitch, or better, reducing the reset operations only to the replacement of die and punches (Fig. 1).

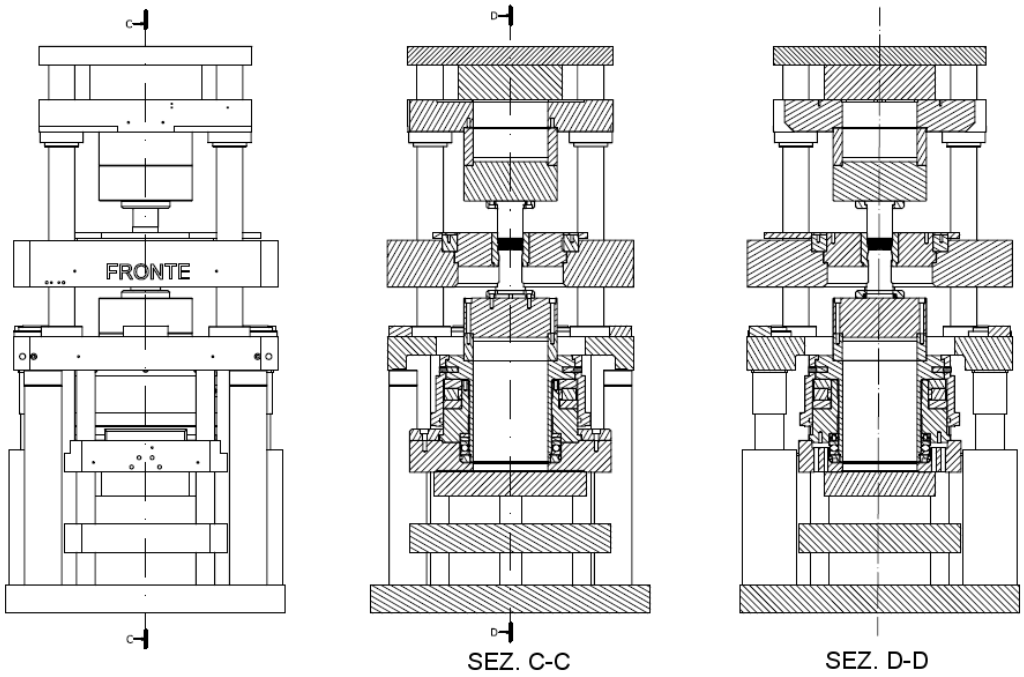

Fig. 1. Pressing system.

For this purpose, a tooling system has been designed, in which the rotary motion of the punch does not depend on a specific component (designed for a specific pitch) but only on the contact between the toothed profiles of die and punches.

The apparatus includes a female die with an inner helical contour, and at least one bottom punch with a contour "perfectly" complementary to the internal profile of the die and corresponding to the helical toothing of the workpiece. An axially movable cover plate carries the die, while the punch is clamped with a lower rotating group. This group is formed by a receiver punch which is clamped with a spacer forming the connecting element between the group and the punch, and two blocks called central fixed block and central mobile block, respectively.

The fixed block is belted by a protection carter and it can only move axially; the mobile block is clamped with the fixed block by a connecting compass and it is connected to the spacer through screws; the difference between the two blocks is that the mobile block is free also to rotate around its axis.

Between the fixed block and the mobile block there is an axial roller bearing appropriately sized to support the load transmitted by the press. This press, hydraulically actuated, is able to apply a maximum load of 200 metric tons and it engages with the central fixed block during the operations giving, thus, the axial motion to the system, which consists by the connecting between punch and upper rotating group and allowing the punch to exert the right pressure on the metal powder contained in the die.

The protection carter, which constitutes the load-bearing element of the couple formed by rotating group and top punch, and the movable cover plate, which constitute the load-bearing element of the die, are housed in driving shafts (forming a prismatic couple allowing axial motion to the system), that, in turn, are clamped on the die base.

Of course, the punch must advance into the die during the operation, so since it has an outer helical contour and the die has the female profile, the punch must necessarily have not only an axial motion but also a rotary motion around its axis. The rotary movement of the punch is obtained by direct cooperation of the helical toothing of the

plunger with the complementary inner contour of the female die which is blocked in the movable cover plate during the powder metal compression; this cooperation starts when the teeth of the punch come in contact with the complementary teeth of the die by means of the axial push of the press. So, the teeth's die "push" the teeth's punch, forcing it to rotate around its axis while the die is stopped. In this way, the teeth's flanks of the punch creep along the teeth's spaces of the die, which behave like a guide.

2.1. Device operations

At the beginning of the operations, the press, the rotating group and consequently the top punch are located in their highest upward position in order to fill the die by the right quantity of powdered metal. For this purpose, the lower part is set with the bottom punch already in the die acting as a base for the powder filling. From this it derives the not perfect symmetry of the system: the punches start from different distances with respect to the center cross section of the die.

Once the die is filled, the hydraulic top press pushes the rotating group and top punch, which begin their axial stroke; in turn, the bottom press pushes the rotating group and bottom punch in order to have always bilateral and symmetrical densification. When the contact between the teeth of the punch and the teeth of the die begins, a rotary motion is added to the axial motion of the plunger, thus, the punch describes a helical trajectory necessarily to advance in the die (this is true for both upper and lower punches). Furthermore, when the plunger starts the rotary motion, consequently also activates the rotation of the components connected to it: punch receiver, spacer, central mobile block. Therefore, it has been necessary to introduce an axial roller bearing to reduce the friction considerably.

When the internally lubricated metal powder reaches the specified average density (that is when the top and bottom plunges end their stroke), the lift cylinders command the ascent of the group and then of the top punch. In this way, the axially movable cover plate moves the die downward to eject the green gear, which is pushed upward thanks to the relative motion between the lower punch (that in this phase is held steady in the axial direction) and the die: the green part, once completely out of the die, is grabbed by a "soft" mechanical arm and the cycle of production restarts.

3. Die geometric parameters

The hydraulic press used to operate the described tooling system is able to apply a maximum load of 200 metric tons. In PM, typical values of the green density are included between 6 and 7.5 g/cm^3, Bocchini (2013). So, it has been chosen a 7.15 g/cm^3 density, corresponding, indicatively, to 590 MPa axial pressure for an atomized (and internally lubricated) iron powder. From this data it is possible to calculate the pitch diameter d_p = 65 mm. By assigning teeth number, z = 50, it is possible to determine all the geometric parameters that define the prototype toothed wheel, with respect to circular module. The assigned parameters, with their values, are reported in the following Table 1:

To complete the definition of the parameters of the die, it is necessary to define the outer insert diameter, D_c, (or the inner ring diameter, d_r) and the outer ring diameter, D_r.

Usually, the α-ratio between the insert diameters d_c and D_c ranges between 0.6 and 0.8. In this case, for the outer insert diameter it has been chosen D_c = 100 mm (by imposing α = 0.65, i.e. neglecting the quite small difference between pitch and outside diameters of the gear). In the same way, it is possible to define a ratio between D_c and D_r (inner and outer ring diameters). In this case, outer ring diameter has been chosen D_r = 300 mm (by imposing $D_c / D_r \approx 0.333$).

The workpiece height, h_p, has been chosen equal to 30 mm; so, the die height (H_m) has been chosen three times greater than h_p, obtaining H_m = 90 mm.

Finally, the die is set in such a way that both punches travel a height of 18 mm within the die. However, at the end of their stroke, due to the not perfect symmetry of the above system, taking as reference the upper surface of the die, the upper punch will have the frontal surface placed at a distance equal to 18 mm and that of the lower punch will be distance equal to 42 mm (90 – 30 – 18 = 42 mm) (Fig. 2).

Table 1. Geometric parameters of the toothing.

Symbol	Meaning	Value
m_c	Circular module	1.3
z	Teeth number	50
p_c	Circular pitch	$p_t = \pi m_c = 4.084$ mm
h_a	Addendum	$h_a = m_c = 1.3$ mm
h_d	Dedendum	$h_d = 1.25 m_c = 1.625$ mm
h	Whole depth	$h = h_a + h_d = 2.25 m_c = 2.925$ mm
d_p	Pitch diameter	$d_p = 65$ mm
d_a	Outside diameter	$d_a = d_p + 2m_c = 67.6$ mm
d_f	Bottom diameter	$d_f = d - 2h_d = 61.7$ mm
δ_c	Pressure angle	$\delta_c = 20°$
d_b	Base circle diameter	$d_b = d_p \cos(\delta_c) = 61.08$ mm
β	Helix angle	β = 5°,18° and 30°
L	Lead	$L = \pi d_p / \tan(\beta)$; L(β =5°) = 2334.057mm; L(β =18°) = 628.474mm; L(β =30°) = 353.691 mm

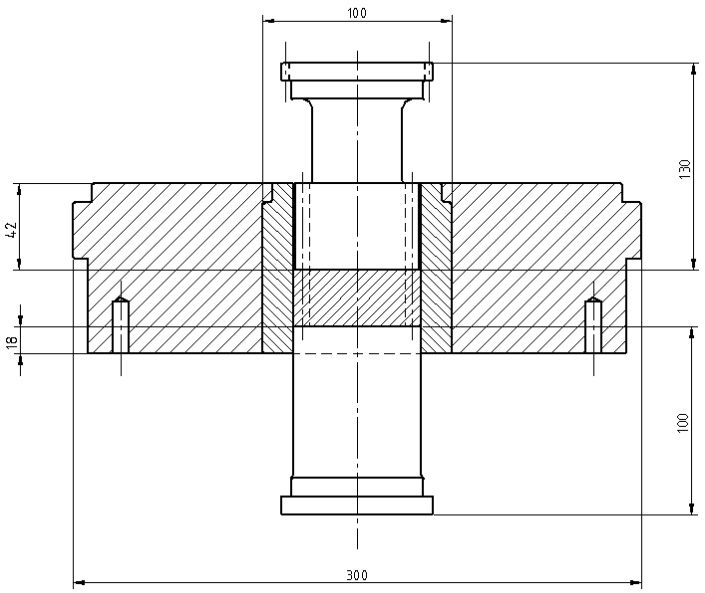

Fig. 2. End-of-stroke die.

Fig. 3 shows the upper punch and the die of the tool produced by Officine Meccaniche Pontillo ($\beta = 18°$).

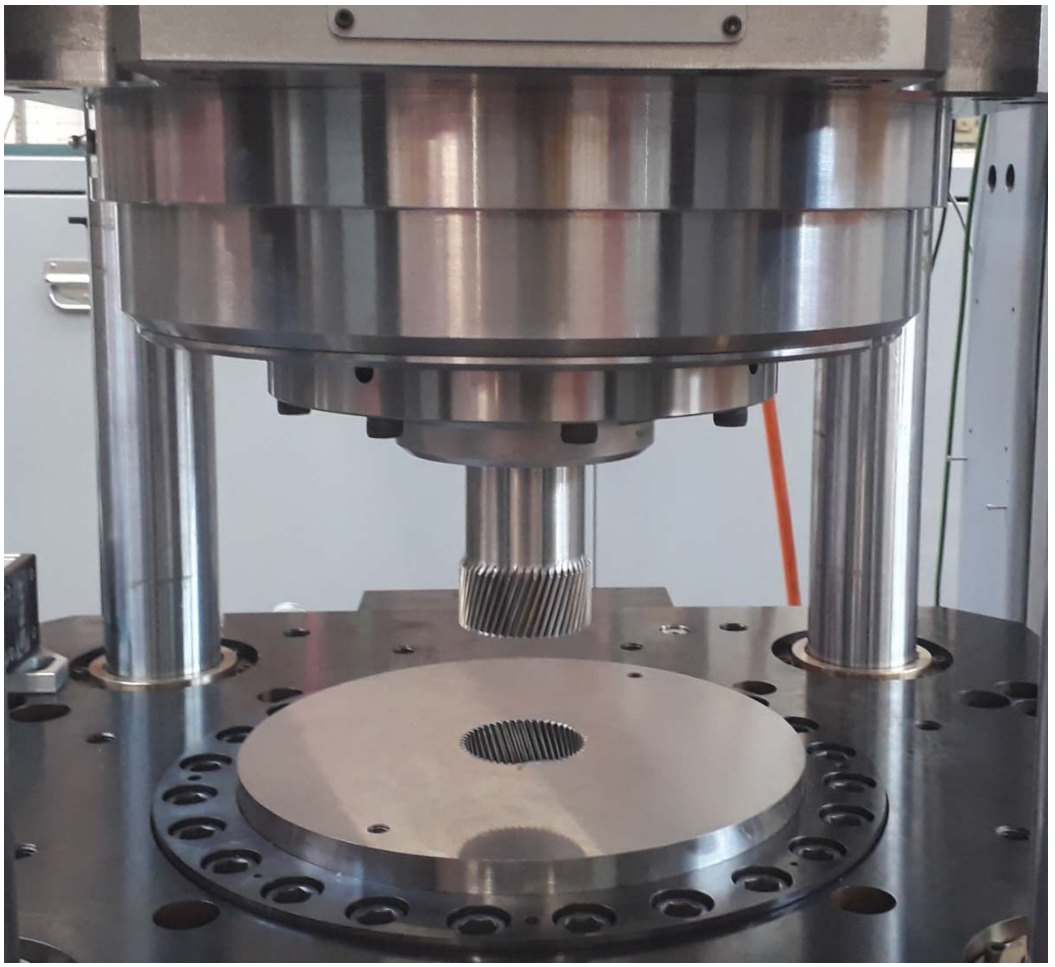

Fig. 3. Upper punch and die of the tool produced by Officine Meccaniche Pontillo (β = 18°).

4. FE model

Three case studies have been analyzed: β = 5°, 18° and 30°.

Because of insert internal profile is helical toothing, the die does not have geometrical symmetry planes; so, it is not possible to consider only a portion of the model to reduce computational times. For this reason, the analysis was carried out using the sub-modeling technique: at first, the analysis must be carried out on the whole model, made of not very dense mesh, then the results of whole model, more properly the displacements, are exploited to conduct the analysis on a sub-model, that is a portion of the whole model, but made of a much denser mesh.

4.1. Generation of tooth, insert and shrink-fitting ring profiles

To generate the helical tooth, first of all the circumferential tooth profile has been generated. Subsequently, it has been extruded following a helical motion obtaining, thus, the helical tooth volume. The same procedure has been also used for the insert and ring profile, obtaining the helicoidal portion of the die (insert plus ring) relative to a single tooth.

The tooth profile is obtained by means of two curves, which are respectively a trochoid arch and an involute arch; the trochoid extends from the bottom circle to the limit circle and the involute from the latter to the outside circle.

The values of the parameters relating to the tooth profile are chosen as shown in Table 1.

The next step has been to create the inside and outside circle sections; the outside arc is equal to half the thickness of the tooth head, while the inside one is equal to half of the existing space on the bottom circle. Subsequently, the involute profile has been connected to the outside circumference by a radius of 0.3 mm, whereas the inside circle is connected to the tooth profile, due to the intrinsic properties of the trochoid (Fig. 4a). The whole tooth profile is obtained by mirroring the obtained half part around the transverse axis of the profile. To create the surface portion of the die relative to the tooth, three circumferential arcs have been generated: one (a, in Fig. 4b) relative to the outer ring profile, and two (b, c, coincident) relative to the external insert and inner ring profile. Finally, the ends of the arcs have been joined with radial segments (Fig. 4b).

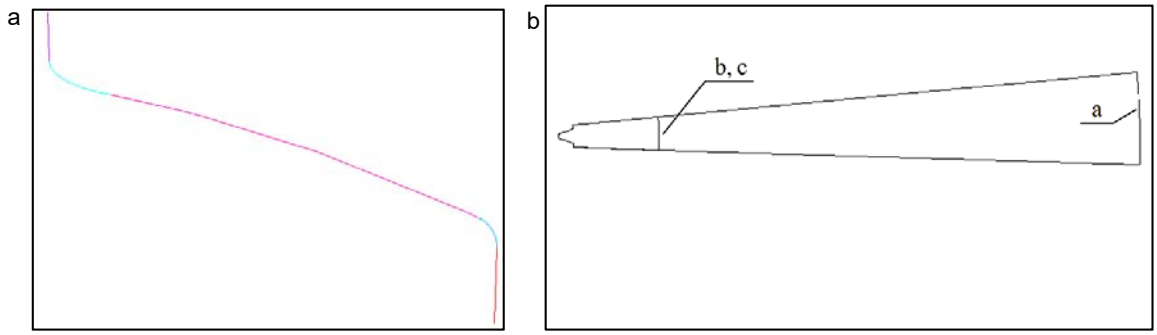

Fig. 4. (a) Half-tooth profile; (b) insert and ring profiles.

4.2. Die generation

To obtain a mapped mesh, made of 20-node hexahedral elements, a plane mesh has been prepared (Fig. 5). Then, the helical tooth is obtained by attributing to the profile both the translation (along z axis) and the rotation (around z axis) (Fig. 6). In the same way, insert and ring portion relative to the realized tooth has been obtained (Fig. 7).

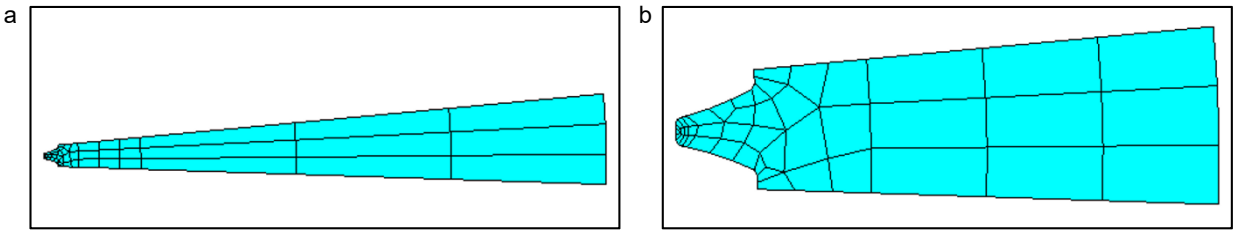

Fig. 5. (a) Mesh of the entire profile; (b) insert mesh.

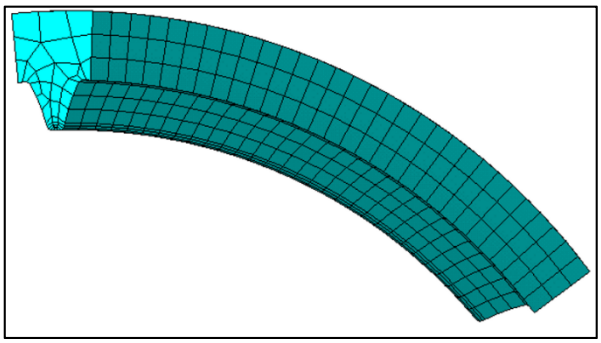

Fig. 6. Top view of tooth mesh.

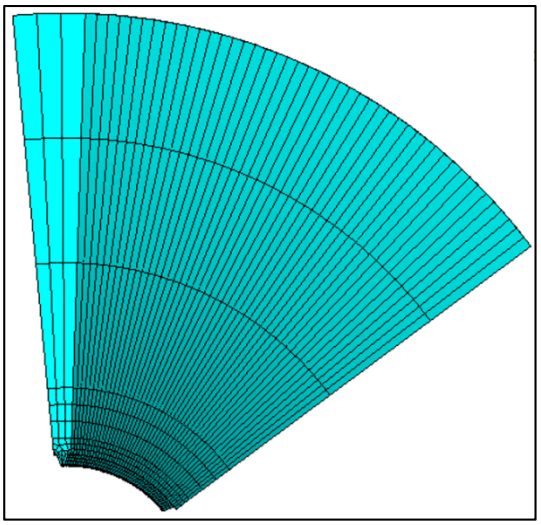

Fig. 7. Insert and ring portion mesh.

Finally, for the die generation, the single helical tooth has been copied z times (in this case z = 50) around z-axis (Fig. 8).

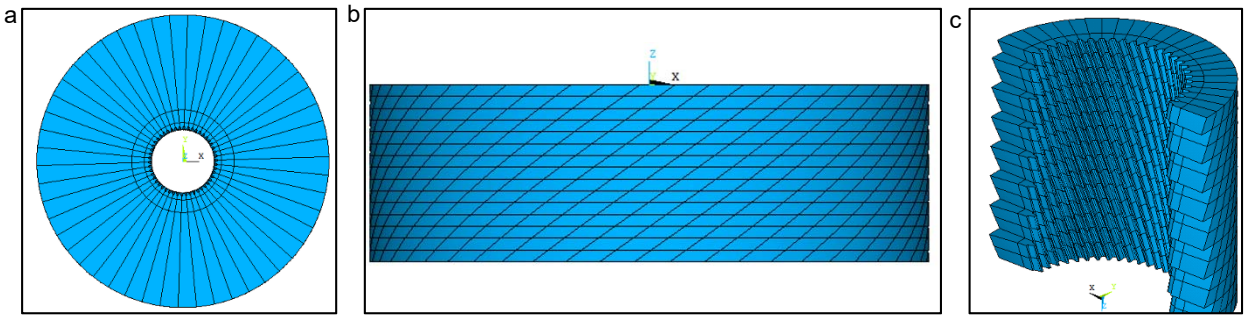

Fig. 8. (a) Die top view; (b) Die lateral view; (c) Sectional view of the insert.

4.3. Materials

The used materials are:

- CPM10V for the die insert;
- hardened and tempered WR 1.2714 for the shrink-fitting ring.

CPM (Crucible Particle Metallurgy) 10V is a new steel produced by the powder metallurgy process. Its composition, w%, is: 9.75% V, 5.25% Cr, 1.30% Mo, 0.90% Si, 0.50% Mn, 2.45% C. It has been designed on a basic analysis of a tough, air-hardening steel with additions of high amounts of carbon and vanadium to achieve an exceptional resistance to wear, toughness and resistance for applications in cold and semi-cold processes. The very high wear resistance and good toughness of the CPM10V make it a candidate for replacing hard metal or other wear-resistant materials in cold working, particularly when the tool must have toughness characteristics with very high wear resistance.

WR 1.2714 (55NiCrMoV7) is a Ni-Cr-Mo steel characterized by high hardenability and toughness, good resistance to repeated shocks, acceptable insensitivity to temperature changes and good resistance to wear.

Table 2 shows the mechanical properties of the selected tool materials.

Table 2. Physical properties, at room temperature, of die materials.

Material	Young modulus [GPa]	Poisson ratio	Thermal expansion coefficient [mm/(mm×°C)×10^6]
CPM10V	228	0.3	12.3
WR 1.2714	215	0.3	13

4.4. Loads

Two loading conditions has been considered:

- the radial pressure due to powder metal at the end of pressing;
- the shrinking pressure exerted on the insert by the ring.

The radial pressure (P_r) acts on the lateral surface portion of the insert of the die, coinciding with the lateral surface of the compact at the end of the compression.

Tests were carried out for the construction of a full prototype in order to make the entire load exerted by the press on the powder. Moreover, the worst load condition was chosen, in which the radial pressure is 60% of the axial pressure (P_a) exerted by the punches on the metal powder:

$$P_r = 0.6P_a \tag{1}$$

From an axial pressure value equal to 590 MPa, we get: $P_r = 0.6 \cdot 590 = 354$ MPa (Fig. 9)

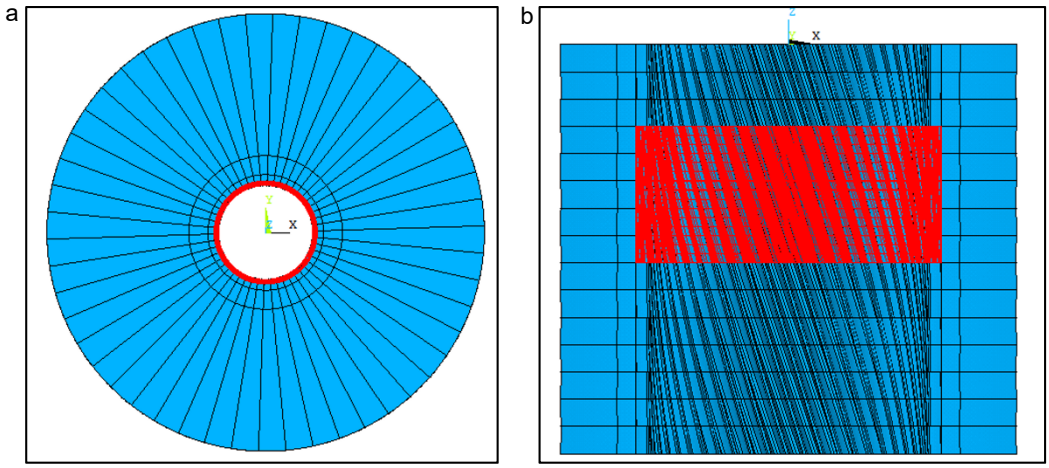

Fig. 9. (a) Radial applied pressure zone for the forming area – axial view; (b) - radial view.

To generate the insert-ring interference a cooling of the shrink-fitting ring has been simulated, as follows:

$$\Delta T = {-\frac{I}{\Phi}}\Big/{\lambda_c} = {-\left(\frac{0.3}{100}\right)}\Big/{(13 \cdot 10^{-6})} \cong -231K \tag{2}$$

where

- (I/Φ) is the relative interference between insert and ring;
- λ_c is the thermal expansion coefficient of the ring material.

4.5. Boundary conditions on global model

Just constraints in order to avoid rigid body motion have been applied: both for the ring and for the insert, 3 appropriate nodes are fixed in axial (z-axis) and tangential direction as show in Fig. 10.

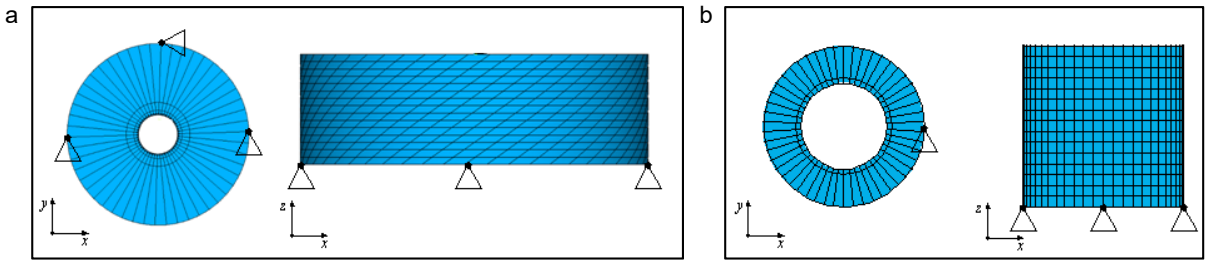

Fig. 10. (a) Constraints at the nodes of the ring; (b) and insert.

4.6. Insert-ring contacts

To simulate the contact between the insert outer surface and the ring inner surface, relative radial constraints have been imposed at the nodes on interface surface, as show in Fig. 11.

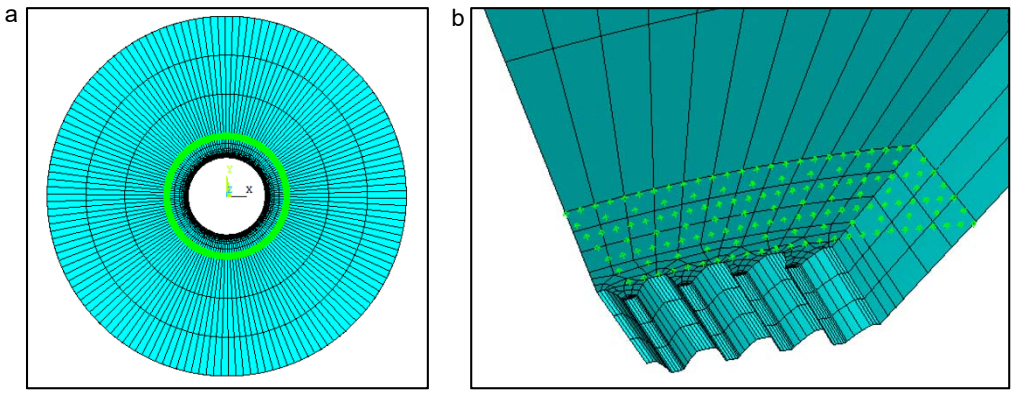

Fig. 11. (a) Constraint Points applied to the interface nodes; (b) detail.

4.7. FE sub-modeling

In order to consider a refined mesh and reduce calculation times, a FEM sub-model of only the region of interest has been built. The same procedure used to generate the whole model has been applied to create the sub-model. A portion large enough to show the helicoidal geometry of the tooth has been chosen. So, while for $\beta = 18°$ and $30°$ a portion of die equal to 1/6 of the entire model was chosen, for $\beta = 5°$ it was sufficient to choose a portion equal to 1/12 of the whole die, obtaining a clear advantage in terms of computational time, without alteration of the final results. Fig. 12 shows the sub-models for the three case studies.

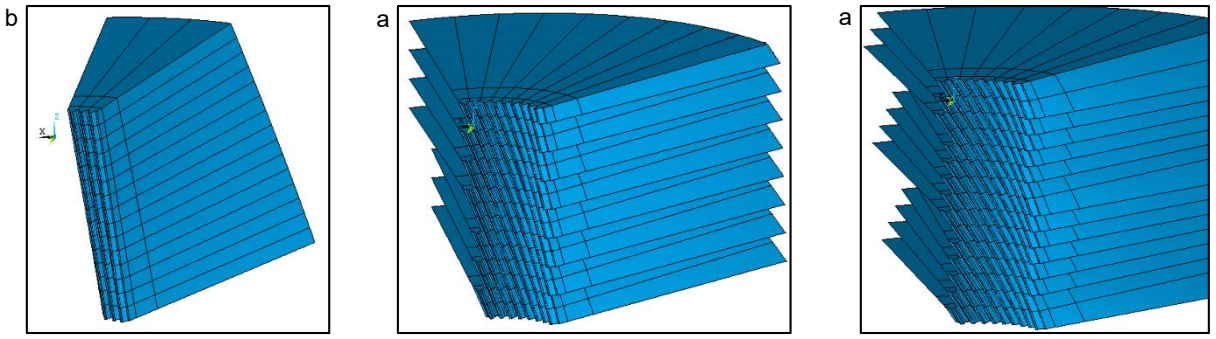

Fig. 12. (a) Sub-model with β = 5°; (b) Sub-model with β = 18°; (c) Sub-model with β = 30°.

For the sub-model, therefore, a more dense and more accurate mesh has been created, in particular the portion relative to the toothing and in correspondence of the connecting radius of the tooth space (Fig. 13). Displacements calculated on the cut boundary of the coarse model have been imposed as boundary conditions for the sub-model, together with the specific external pressure.

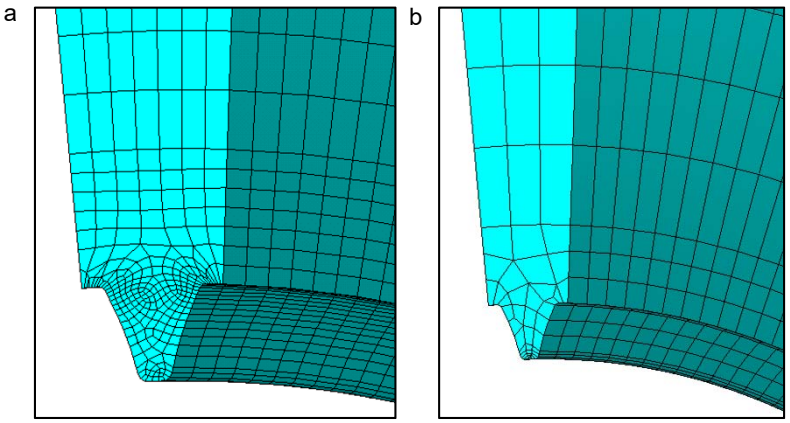

Fig. 13. Comparison between the mesh of a sub-model tooth (a) and of the whole die (b).

5. Results analyses

Analyses have been conducted for the three different case studies, β = 5°, 18° and 30°. Results are reported in terms of stress states and displacements, for the combined loads of shrinking and radial pressure.

Fig. 14 shows Maximum Principal Stresses for the case β = 5° for the insert; the maximum tensile value (S1 = 263 MPa > 0) is modest and is present along the active tooth profile. On the contrary, in the upper and lower areas of the insert, with respect to the forming zone, compression stresses are always present. Instead, the highest compression stresses (maximum value S3 = -1531 MPa < 0) occur in correspondence of the outside fillet radius of the gear, in the lower part of the matrix. Maximum compression stresses are principally circumferential stresses. The maximum compression values are found far from the forming zone and only in the lower part of the die, due to the load asymmetry in axial direction. The forming pressure, which generates strong tensile stresses, tends to balance the compression stresses due to the shrinking that are located in the lower area far from the action of the powder pressure.

Fig. 15 shows Von Mises stresses on the ring. In this case, the circumferential stresses are exclusively tensile, while the radial ones are exclusively compression.

Fig. 16 shows both the radial and circumferential displacements, which can have great influence on compact ejection. Maximum values in radial direction are located in the central area of the die where pressure acts during the forming. The maximum displacements in the circumferential direction occur, instead, along the active profile of the tooth and – luckily – they are negligible (less than 5 μm).

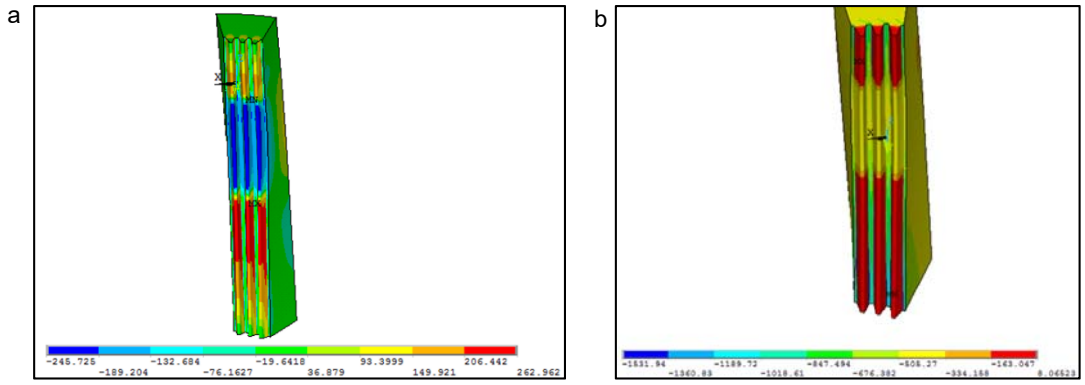

Fig. 14. Maximum Principal Stresses [MPa] in the insert. (a) Tensile stresses - (b) Compression stresses.

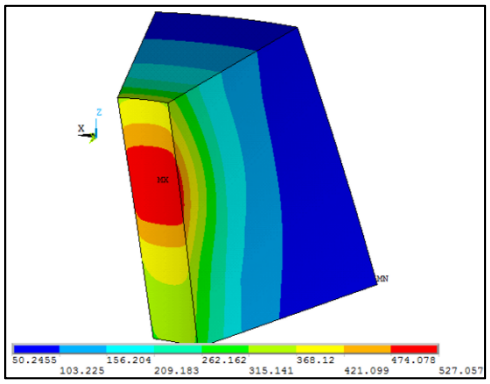

Fig. 15. Von Mises stresses in the ring at compaction end [MPa].

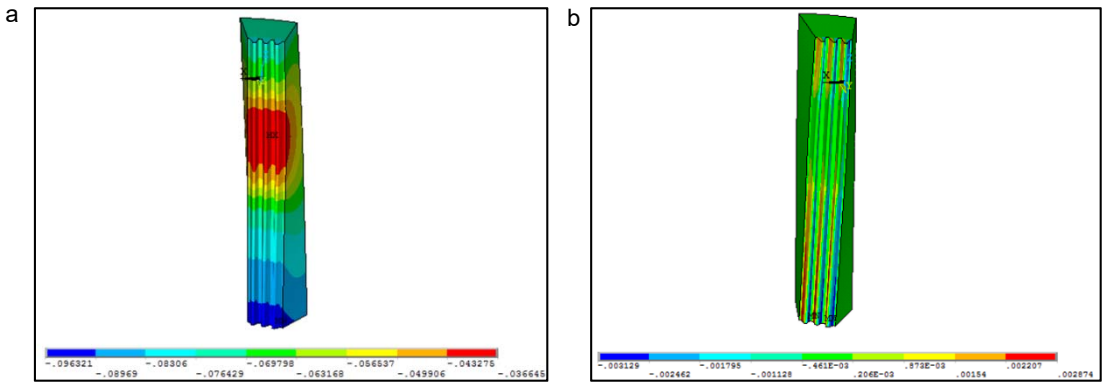

Fig. 16. (a) Radial and (b) circumferential displacements of the insert [mm].

Similar contour plots are obtained for the case β = 18° and 30°, with the same shrinking and radial pressures; the stress conditions and displacements relative to insert and ring do not change. Fig. 17 shows Maximum Principal Stress in the insert for the cases β = 5°, 18° and 30°; whereas Table 3 shows both the radial and circumferential displacements.

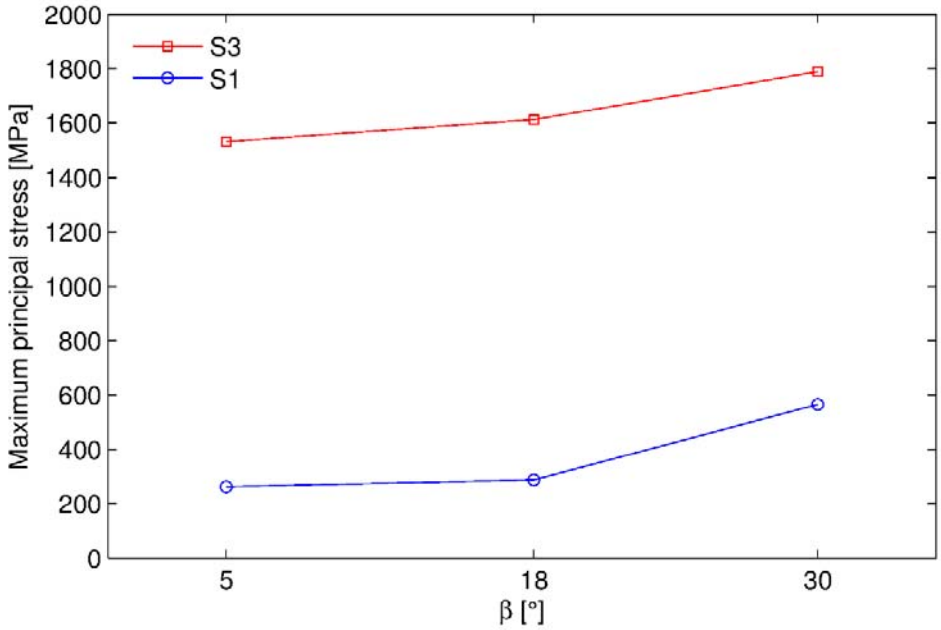

Fig. 17. Maximum Principal Stress [MPa] in the insert versus β-values. (S1) Tensile stresses - (S3) Compression stresses (absolute value).

Table 3. Maximum displacements of the insert (U_x are in absolute value).

Displacement [mm]	β = 5°	β = 18°	β = 30°
U_x	0.096321	0.095394	0.093696
U_y	0.003129	0.003682	0.005358

It can be observed that the stresses increase with the helix angle associated with the increasing of the lateral surface on which the forming pressure acts. In any case, the maximum values are lower than the yield stress of the material (2460 MPa) ensuring the absence of plastic deformations.

In all the cases analyzed, the maximum stress values are located at the fillet radius of the tooth die space and occur in the lower part of the die, where the tensile effects due to the forming pressure are extinguished.

The values of the radial displacements are very similar for the three cases: the maximum values (in absolute value) occur on the lower part of the insert and derive from the action of the shrink-fitting ring. The circumferential displacements are practically negligible in all the case studies. Displacement values are particularly important in order to avoid problems during the compact ejection (blockage of the green part inside the die).

Finally, it is noted that the maximum radial compression stress acting on the ring is equal to about 350 MPa. This value corresponds to the shrinking pressure. It is necessary to investigate the possibility of slippage of the core during the extraction of the piece. The friction force generated by the shrinking pressure must be greater than the extraction force exerted by the lower punch. Applying equilibrium equations, it is possible to determine analytically the maximum helix angle to avoid axial slip-off of the core: the maximum value is β = 45°. This result is valid for the value of the considered interference and radial pressure and it ensures the absence of slip-off phenomena during the ejection of green helical gears with helix angles in the range of interest, namely from 0° to 30°.

6. Conclusions

The treatment of the punch-die system as a self-locking screw has encouraged experimentation with limited angles of the range of interest. The results of the experimental tests have been excellent and the numerical analysis to the software confirmed that even for larger angles there should not be problems related to the resistance of the materials. Typical (happily not frequent) PM compaction problems, such as blocking of the formed part into the die, or slippage of the insert from the shrink-fitting ring are avoided. In particular, for the latter, it has been seen that the system should operate with good safety up to 30° without the aid of additional components that help the rotation of the punch.

In this regard, tests have been carried out with a tool for making helical gears with an 18°-helix angle, but with a maximum load of 60 tons exerted by press and with the aid of a insert plunger for the realization of the gear bore. In this case also, after 20000 cycles, the system has showed no problem whatsoever: the punch and die toothings did not show any wear; the punch has always slipped correctly inside the die; no problems related to the insert or piece slip-off occurred during the extraction of the same, with the interference value established.

These results encourage the possibility to realize a tool with the established parameters, able to form any helix angle without the aid of additional components.

In the future, it will be possible to carry out experimental tests and perform dynamic numerical analyzes to verify effectively the limit of the tool in terms of useful life related to wear and fatigue resistance of the materials considered.

References

Armentani, E., Bocchini, G.F., Cricrì, G., Esposito, R., 2002. Short dies and thin-walled insert for room temperature or warm compaction - numerical determination of design features. Powder Metallurgy 45, 115–133.

Armentani, E., Bocchini, G.F., Cricrì, G., Esposito, R., 2003. Metal powder compacting dies: optimised design by analytical or numerical methods. Powder Metallurgy 46, 349–360.

Armentani, E., Bocchini, G.F., Cricrì, G., Esposito, R., 2007. Warm compaction: FEM analysis of stress and deformation states of compacting dies with rectangular profile of various aspect ratio. Materials Science Forum 534, 329–332.

Armentani, E., Bocchini, G.F., Cortigiano, A., Cricrì, G., Esposito, R., 2008. FEM analysis of stress and deformation states of shelf dies for metal powder compaction. Advances in Powder Metallurgy & Particulate Materials, 52–63.

Armentani, E., Bocchini, G.F., Cricrì, G., 2012. Doubly shrink fitted dies: optimisation by analytical and FEM calculations. Powder Metallurgy 55, 130–141.

Armentani, E., Bocchini, G.F., Cricrì, G., 2013. Compaction dies for spur gears: FEM analysis to assess the influence of some design parameters on stress state. Metallurgia Italiana 105, 11–22.

Bocchini, G.F., 2013. Compressibility curves of iron-base powders: Reliable or insidious references for a correct preliminary evaluation of stresses on compaction tools?. Metallurgia Italiana 105, 3–19.

Cricrì, G., Perrella, M., 2016. Modelling the mechanical behaviour of metal powder during die compaction process. Frattura ed Integrità Strutturale 10, 333–341.